
FIGARO: Generating Symbolic Music with Fine-Grained Artistic Control

Dimitri von Rütte¹ Luca Biggio¹ Yannic Kilcher¹ Thomas Hofmann¹

Abstract

Generating music with deep neural networks has been an area of active research in recent years. While the quality of generated samples has been steadily increasing, most methods are only able to exert minimal control over the generated sequence, if any. We propose the self-supervised *description-to-sequence* task, which allows for fine-grained controllable generation on a global level. We do so by extracting high-level features about the target sequence and learning the conditional distribution of sequences given the corresponding high-level description in a sequence-to-sequence modelling setup. We train FIGARO (FIne-grained music Generation via Attention-based, RObust control) by applying *description-to-sequence* modelling to symbolic music. By combining learned high level features with domain knowledge, which acts as a strong inductive bias, the model achieves state-of-the-art results in controllable symbolic music generation and generalizes well beyond the training distribution.

1. Introduction

Music is a fascinating subject that surrounds us constantly, being a source of inspiration and canvas for imagination to many. To some, creating music is a topic worthy of dedicating one’s life to, which is a testament to the artistry and mastery involved. While composition is an intricate form of art that requires a deep understanding of the human experience, the idea of devising a systematic or algorithmic approach to music creation has been around for centuries (Nierhaus, 2009).

With the advent of deep learning, automatic music generation has seen renewed interest (Hernandez-Oliván & Beltrán, 2021). Especially the Transformer architecture (Vaswani et al., 2017), popularized in the context of Natural Language processing (Brown et al., 2020) and then successfully ap-

plied in several other Machine Learning tasks (Dosovitskiy et al., 2021; Lample & Charton, 2019; Biggio et al., 2021), has proven to be a powerful tool for musical sequence modelling. Initial breakthroughs by Huang et al. (2018) and Payne (2019) applied language modelling techniques to symbolic music to achieve state-of-the-art music generation. These models featured limited controllability, if any, and subsequent work attempts to improve on this limitation through various avenues (Ens & Pasquier, 2020; Choi et al., 2020; Wu & Yang, 2021; Hadjeres & Crestel, 2020).

As deep generative models are improving and producing more and more realistic samples, it remains an area of active research how humans can interact with these models and get them to generate a desirable result. Recent efforts in text-to-image generation (Ramesh et al., 2021) have shown the potential in usability and artistic applications of human-interpretable controllable generative models. However in contrast to image modelling, controllable sequence modelling appears to be more challenging: On one hand, it is unclear how to incorporate meaningful attributes into the generation process in a way similar to style-based image generation methods (Karras et al., 2019). On the other hand, it is difficult to find meaningful attributes in the first place, as obtaining salient features for discrete data such as text or in this case symbolic music can be prohibitively difficult or expensive (Shao et al., 2008; Ens & Pasquier, 2019).

Our key contribution consists of a novel self-supervised task for training conditional sequence models at scale. We call this the *description-to-sequence* task and apply it to the domain of symbolic music to demonstrate that it is effective at enabling controllable symbolic music generation. The goal of our work is to provide *global yet fine-grained control* over the generation process such that the user is able to define a guideline, some form of high-level instruction for the whole piece, which is subsequently interpreted and implemented by the model at generation time. We propose the *description-to-sequence* task where a high-level description is extracted automatically from a given sequence and the model learns to reconstruct the original solely based on the description. To this end, we define the *description function* as a function that, taking as input a single bar of music, defines a set of descriptive features for that bar. Concatenating the features of each bar results in a sequence of events describing the entire piece. In order to train FIGARO

¹Department of Computer Science, ETH Zürich, Zürich, Switzerland. Correspondence to: Dimitri von Rütte <dvrutte@ethz.ch>.

FIGARO: Generating Symbolic Music with Fine-Grained Artistic Control

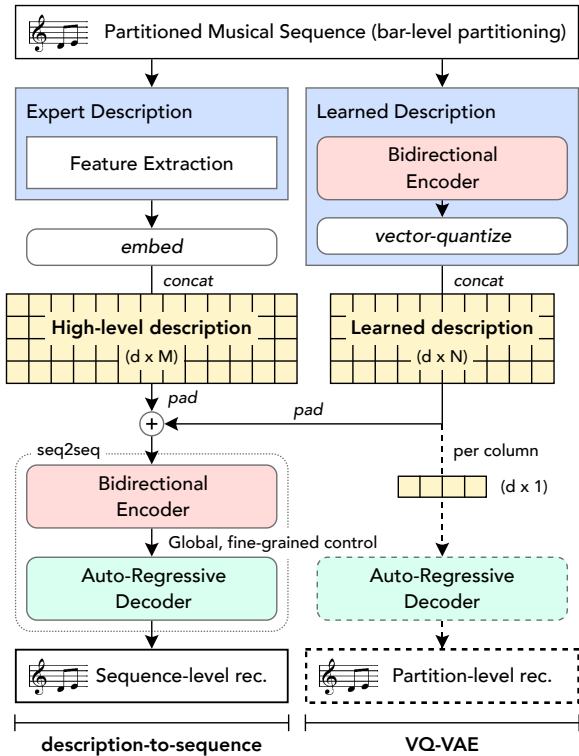


Figure 1. Overview of FIGARO. Dashed lines indicate components that are only used during training. d denotes the hidden dimension of the model, N the number of bars and M the length of the expert description ($M > N$ in our case).

by applying *description-to-sequence* modelling to symbolic music, we propose two different description functions: 1) The hand-crafted *expert* description, which provides global context in the form of a low-fidelity, human-interpretable sequence and 2) the *learned* description, where we use representation learning to extract high-fidelity salient features from the source sequence. Once trained in this way, our model can be employed to generate music given a description encoding the salient features of the target song. If the description is sufficiently interpretable and detailed, this procedure allows for globally human-controllable music generation at a fine-grained scale.

We evaluate the proposed method on its ability to adhere to the prescribed condition by comparing it to state-of-the-art methods for controllable symbolic music (Choi et al., 2020; Wu & Yang, 2021). We demonstrate empirically that our technique outperforms the state-of-the-art in controllable generation, modelling capability and sample quality. To evaluate sample quality, we employ subjective evaluation in the form of a user study. We further demonstrate that our models are robust and generalize well by evaluating the zero-shot performance on out-of-distribution data, indicating that the proposed *description-to-sequence* task is effective at learning generalized high-level concepts about the data.

The paper is structured as follows: First, we provide an overview of existing work and compare the level of controllability of different generative models. Next, we introduce the *description-to-sequence* modelling task and describe our method by applying the task to symbolic music. We then perform a quantitative evaluation of our models compared to state-of-the-art methods on conditional generation and zero-shot performance. We also perform an ablation study to validate different parts of the proposed model and finally evaluate the subjective quality of generated samples.

2. Controllable Symbolic Music Generation

We identify two different levels of controllability over the generation process. The most prevalent form of control is global conditioning of the model, where the generation is guided by a constant set of attributes which do not change during the generation process. Examples of global control include prompt-based conditioning (Payne, 2019) or conditional decoding of latent representations (Brunner et al., 2018). Fine-grained control is achieved when the generation process can be guided at any point in time, i.e. if the control attributes can be arbitrarily varied over time. Consider controlling what instruments are playing in the generated sequence as an example of global control in contrast to controlling what instruments are playing *at any point in time* as an example of fine-grained control. Note that fine-grained control also implies global control, as global control can be achieved by fixing the control attributes to some constant value. Fine-grained control is therefore a strictly more powerful property and seemingly harder to obtain, as is highlighted in Table 1.

2.1. Related Work

The capabilities of symbolic music generative models have been steadily improving with notable contributions by Huang et al. (2018), Payne (2019), Huang & Yang (2020) and Hsiao et al. (2021). This line of work focuses on improving the quality of generated samples but does not contribute substantially toward controllable generation. An exception to that is MuseNet (Payne, 2019), which allows some control through prompt-based conditioning with control tokens. Even still, prompt-based control is very limited, as control tokens are “forgotten” by the model once the generation advances beyond the initial context size.

Another line of work focuses on finding ways of controlling the generation process. Brunner et al. (2018) propose MIDI-VAE as a method for conditional generation as well as genre transfer between pop and jazz music. Choi et al. (2020) introduce a method for generating melody-conditioned piano performances. Ens & Pasquier (2020) present MMM which is capable of bar-level and track-level symbolic music inpainting. Hadjeres & Crestel (2020) propose VQ-CPC

FIGARO: Generating Symbolic Music with Fine-Grained Artistic Control

Method	Input Rep.	Multi-Track	Multi-Sig.	Global Ctrl.	Fine-Grained Ctrl.
MIDI-VAE (Brunner et al., 2018)	Pianoroll	✓	✓	✓	-
MuseNet (Payne, 2019)	MIDI-like	✓	✓	(✓) ¹	-
MMM (Ens & Pasquier, 2020)	MIDI-like	✓	✓	✓	-
Choi et al. (2020)	MIDI-like	-	✓	✓	(✓) ²
VQ-CPC (Hadjeres & Crestel, 2020)	Lead sheet	-	-	✓	✓
MuseMorphose (Wu & Yang, 2021)	REMI	-	-	✓	✓
FIGARO (ours)	REMI+	✓	✓	✓	✓

Table 1. Generative capability and controllability comparison between different methods proposed in the literature. We compare our method to other state-of-the-art symbolic music generation methods on modelling capability (can the model generate multi-track/multi-signature music?) and controllability (can the generation be controlled on a global/fine-grained level?). We omit Huang et al. (2018), Huang & Yang (2020) and Hsiao et al. (2021) as they are strictly less capable in terms of controllability than other work in the comparison.

¹ While it is possible to control the style (via artist tags) and instruments of the generated sequence, this information is “forgotten” by the model due to context scrolling once the generation advances beyond the initial prompt.

² Fine-grained control is limited to optionally prescribing the melody of the generated sequence.

for generating novel variations on existing music. Finally, Wu & Yang (2021) introduce MuseMorphose for attribute-based conditional generation and style editing. All of these approaches have various limitations that are highlighted in Table 1. Common simplifications include limiting the model to a single track and the 4/4 time signature. Either of these simplifications and in particular the combination of both severely limit the real-world applicability of resulting models, as most music does not satisfy these assumptions. Both of these limitations are remedied in our work by using appropriate extensions to the input representation.

Fine-grained control has been a topic of interest in the recent literature (Choi et al., 2020; Hadjeres & Crestel, 2020; Wu & Yang, 2021; Di et al., 2021; Ferreira & Whitehead, 2021) and is an essential property when considering user-directed applications. In essence, fine-grained control is necessary to allow control over salient features in the generation, as saliency in music at least partly lies in how it changes over time. In addition, salient features may be impossible or prohibitively expensive to quantify (Choi et al., 2020; Ferreira & Whitehead, 2021), emphasizing the need for un- or self-supervised fine-grained control. Our proposed method provides both global and fine-grained control through description-to-sequence modelling.

3. Description-to-Sequence Modelling

3.1. Description Function

The goal of our method is to define a descriptive conditioning sequence \mathbf{d} on a high level and train a generative model that learns the data distribution conditioned on \mathbf{d} , i.e. $p(\mathbf{x}|\mathbf{d})$.

To this end, let \mathcal{X} be a distribution of sequences and let $\mathbf{x} \sim \mathcal{X}$. Let p_1, \dots, p_n denote a partition of \mathbf{x} into a finite number of sub-sequences, such that $\mathbf{x} = p_1 \parallel \dots \parallel p_n$ with \parallel denoting concatenation. We define the description

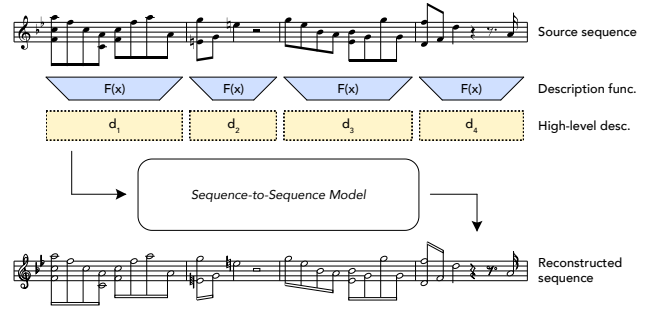


Figure 2. Schematic overview of the proposed description-to-sequence task.

function $F(\cdot)$ as a function that takes the i -th element of the partition p_i over a finite vocabulary V_{seq} as the input and returns another sequence d_i over a finite vocabulary V_{desc} , which we call the description of p_i . Note that $|p_i| \neq |d_i|$ in general. A useful description function should extract high-level features about p_i , aiding in the reconstruction of p_i in an eventual down-stream task. Given F and \mathbf{x} , we call $\mathbf{d} = F(p_1) \parallel \dots \parallel F(p_n)$ the description of \mathbf{x} . For simplicity, we write $\mathbf{d} = F(\mathbf{x})$ in the following.

3.2. Description-to-Sequence Task

In order to learn the conditional distribution $p(\mathbf{x}|F(\mathbf{x}))$, we minimize the cross-entropy reconstruction loss

$$\mathcal{L}_{\text{rec}}(\phi) = \mathbb{E}_{\mathbf{x} \sim \mathcal{X}} [-\log p_{\phi}(\mathbf{x}|F(\mathbf{x}))],$$

where \mathcal{X} is the true distribution of sequences and ϕ are the parameters of a sequence-to-sequence model. Intuitively, F can be viewed as an information bottleneck: it removes some information about \mathbf{x} but should leave enough for the model to reconstruct the original sequence as accurately as possible. We call this self-supervised setup the *description-to-sequence* task. An illustrated overview is given in Figure 2.

We propose two different description functions for generating descriptions from musical sequences. The first is a hand-crafted algorithm, where we aim to extract *human interpretable* descriptions. This will enable artist-guided creation or editing of descriptions and we refer to it as the *expert* description. In an attempt to improve on the expert description by using learning-based methods, we also propose a second version, which we call the *learned* description. In this case we learn latent representations of given partitions using the VQ-VAE framework (Oord et al., 2018). In both cases we partition \mathbf{x} into its bars b_1, \dots, b_n as this is a natural way to partition musical sequences.

3.3. Expert Description

As a baseline and proof-of-concept, we use domain knowledge to construct a description function that is human-interpretable and could be created from scratch by a human expert. We include trivially important features such as time signature, instruments and chords, as well as stylistically relevant features identified by previous work (Choi et al., 2020).

- Time signature: the time signature of the current bar. By convention, any bar has exactly one associated time signature.
- Note density: the number of note onsets per quarter note
- Mean pitch: average pitch of all note onsets in the given bar
- Mean velocity: average velocity of all note onsets in the given bar
- Mean duration: average duration of all notes with onsets in the given bar
- Instruments: list of all instruments that have note onsets in the given bar
- Chords: list of all chords being played during the given bar

All of these quantities are easy to understand for humans given the necessary domain knowledge. Since the quantities are efficiently computable, pairs of corresponding musical sequences and descriptions are easy to generate. For tokenization, we discretize real values (note density, mean pitch/velocity/duration) to some appropriate interval, ensuring a finite vocabulary. Chords are extracted with an adapted version of the Viterbi algorithm also used by Huang & Yang (2020). An example description is given in Figure 3. More details on feature extraction and tokenization can be found in Appendix B.

3.4. Learned Description

While the expert description serves as a human-interpretable, strong inductive bias, it has various shortcomings. For ex-

```

<bos>
Bar_1 TimeSignature_4/4 NoteDensity_3
      MeanPitch_14 MeanVelocity_19 MeanDuration_32
      Instrument_Drums Instrument_Piano
      Instrument_E-Piano Instrument_SlapBass
      Chord_E:maj Chord_F#:min7
Bar_2 TimeSignature_4/4 NoteDensity_3
...
<eos>

```

Figure 3. Example of an expert description. The description contains information about time signature, note density, mean pitch, velocity and duration as well as which instruments and chords are played throughout the bar.

ample, it is only able to capture fairly low-fidelity features by design and suffers from non-injectivity (i.e. there can be many sequences that map to one description). In an attempt to improve on these points, we use representation learning to extract features that describe the underlying sequence in more detail. We choose the VQ-VAE framework as the basis for our learned description function as it has been shown to be effective for various tasks such as image generation (Oord et al., 2018), speech-recognition (Baevski et al., 2019) and most importantly music generation (Dhariwal et al., 2020). We essentially trade human-interpretable for a higher-fidelity representation.

We embed each partition into a latent vector \mathbf{z}_e , which is then discretized to 16 separate codes with a codebook size of 2048. We use the latent codes given by the VQ-VAE as the learned description function in our experiments. To ensure stable training and reduce the number of trainable parameters, we reuse the frozen embedding weights of the VQ-VAE, effectively feeding the quantized latent embeddings \mathbf{z}_q directly into the sequence-to-sequence model.

4. Method

We train FIGARO by applying the *description-to-sequence* task to symbolic music. We extract bar-level features by using the *expert* and *learned* description functions and feed them into a Transformer auto-encoder trained on reconstruction. We also train FIGARO (expert) and FIGARO (learned), each using only the description indicated in parentheses. An illustrated overview of our method can be found in Figure 1.

4.1. REMI+ Input Representation

To make event-stream-based MIDI input files machine-interpretable, we extend the beat-based revamped MIDI (REMI) representation (Huang & Yang, 2020) to make it suitable for our modelling task. REMI represents notes with four consecutive tokens encoding note position, pitch, velocity and duration. It additionally also includes chord and tempo events to further guide the modelling process.

As first introduced, REMI does not allow for modelling multiple tracks or multiple time signatures. To alleviate this

limitation we propose REMI+, an extension to REMI that makes it suitable for general multi-track modelling tasks. More details on this are given in Appendix A.

4.2. Description-to-Sequence Model

For our description-to-sequence model we stick very close to the original Transformer auto-encoder proposed by Vaswani et al. (2017). Unless specified differently, we use the same hyperparameters as the original paper. To save on computation and training time, we use a context size of 256 tokens in all of our experiments. In the same spirit, we also reduce the number of encoder layers to 4 but leave the number of decoder layers at 6. In total, the description-to-sequence model has 44.6 M trainable parameters.

We use relative positional embeddings (Huang et al., 2020) as this has been shown to be beneficial for symbolic music generation (Huang et al., 2018). In addition to the positional embeddings, we also add a learned bar embedding and a learned beat-position embedding. In the case of using both descriptions, we simply add their embeddings before passing it to the encoder.

Training. We train this model on $(F(\mathbf{x}), \mathbf{x})$ data pairs where \mathbf{x} is a REMI+ sequence and $F(\mathbf{x})$ is either the expert or learned description of \mathbf{x} as described in Section 3. We minimize the cross-entropy reconstruction loss as our training objective.

4.3. VQ-VAE Model

For our VQ-VAE model, we use a 4-layer Transformer encoder in combination with a 6-layer Transformer decoder with cross-attention. The final layer of the encoder is pooled as proposed by Devlin et al. (2019) and projected to the latent space. The latent vector then is discretized and fed to the decoder through cross-attention. The output of the decoder is the PDF $p(x_t|x_{<t})$ for each position in the context. We use a linear layer before and after vector-quantization to project between model space and latent space. The VQ-VAE model has 43.7 M trainable parameters in total.

We use a modified version of the sliced vector quantization scheme proposed by Kaiser et al. (2018) as our discretization bottleneck. Specifically, we decompose the latent representation \mathbf{z} into 16 slices $\mathbf{z}_1, \dots, \mathbf{z}_{16}$ and discretize each of them to a shared codebook \mathcal{C} with $|\mathcal{C}| = 2048$ using the k -means discretization technique from the original paper (Oord et al., 2018).

Training. The model is trained by minimizing the canonical β -VQ-VAE loss without the auxiliary codebook loss (Oord et al., 2019) with $\beta = 0.02$ in all of our experiments. The codebook is updated using the EMA update step as proposed in the original paper. We employ random restarts (Dhariwal et al., 2020) to ensure optimal codebook usage.

5. Experimental Setup

5.1. Dataset

We use the LakhMIDI dataset (Raffel, 2016) as training data in all of our experiments, which to the best of our knowledge is the largest publicly available symbolic music dataset. We use a 80%-10%-10% training-validation-test split. For evaluation, we generate samples conditioned on descriptions sampled from the test set for 24 hours on 8 Nvidia GTX 2080 Ti GPUs, generating 32 bars for each sample. We provide a non-cherry-picked collection of samples and encourage the reader to get an impression of the quality and diversity of the music by listening to some of them.¹

5.2. Training Details

Unless specified differently, we use the following training setup in all of our experiments. We train each model for 100k steps with a batch size of 512 sequences. Models are optimized using the Adam optimizer (Kingma & Ba, 2017) with $\beta_1 = 0.9$, $\beta_2 = 0.999$, $\epsilon = 10^{-6}$ and 0.01 weight decay. We use the inverse-square-root learning rate schedule with initial constant warmup at 10^{-4} given by $10^{-4} / \max(1, \sqrt{n/N})$ where $N = 4000$ is the number of warmup steps. We additionally release the source code and pre-trained model weights that were used in our experiments for additional details on training and hyperparameters.²

5.3. Evaluation Metrics

5.3.1. FLUENCY

We use perplexity (PPL) as a way to measure fluency and to compare the likelihood of different models in addition to task-specific metrics. The perplexity measures the likelihood of sequences while normalizing over the sequence length, which makes it better suited to comparing sequences of different lengths than the negative log-likelihood.

5.3.2. DESCRIPTION FIDELITY

We also quantitatively evaluate the fidelity of generated sequences to the given condition. Let \mathbf{x} denote a test sample and $F(\mathbf{x})$ its description. Then we generate $\hat{\mathbf{x}}$ by sampling the model conditioned on $F(\mathbf{x})$ and examine \mathbf{x} and $\hat{\mathbf{x}}$ for similarity. Metrics are computed as an empirical estimate over the test distribution. More details and exact formulas are given in Appendix C.

Accuracy. We compute accuracy metrics for categorical values, namely for instruments, chords and time signature. Instruments and chord are multi-label features for which we compute the mean F_1 score. We compute the mean accuracy

¹Samples are available on [Soundcloud](#).

²Source code and model weights are available on [GitHub](#).

for time signatures, as there is exactly one time signature per bar by the definition of REMI+.

Macro Overlapping Area. Previous work has used the overlapping area (OA) metric to quantify similarity between two musical sequences for a given feature (Choi et al., 2020; Wu & Yang, 2021). However, we find that the standard OA metric fails to take the order of the sequences into account, as feature histograms are computed over the entire sequence.

To alleviate this limitation, we propose the macro overlapping area (MAO), which partition-wise computes the overlap in the distributions of a given feature, taking sequential order into account. We use the MOA metric to compute similarity in pitch, velocity and duration between ground truth and reconstruction.

Normalized Root-Mean-Square Error. We compute the normalized RMSE (NRMSE) for bar-wise note density. This helps compare similarity across different feature magnitudes.

Cosine Similarity. We also evaluate chroma and grooving similarity as a way to quantify similarity in sound and rhythm as proposed by Wu & Yang (2021). We compute bar-wise cosine similarity for the chroma vectors (Fujishima, 1999) and grooving vectors (Dixon et al., 2004).

6. Experiments

6.1. Conditional Generation

We compare the conditional generative capabilities of our models to an unconditional baseline based on Huang et al. (2018) as well as two state-of-the-art methods for controllable generation (Choi et al., 2020; Wu & Yang, 2021). The unconditional baseline acts as a sanity check: It has no additional information about the source sequence and essentially its output can be seen as a draw from the data distribution, provided training was successful. Choi et al. (2020) and Wu & Yang (2021) get the unmodified target sequence as input while FIGARO gets both descriptions as input. We also train FIGARO (expert) and FIGARO (learned) models, which only get the expert or learned description as input. More details on implementation and training of the benchmarked models can be found in Appendix D.

Perhaps unsurprisingly, FIGARO (expert) performs very well on all metrics that are directly present in the expert description. It also performs reasonably on chroma and grooving similarity, both of which are not directly present in the expert description. This shows that the expert description can act as a strong inductive bias and helps guide the generation process even beyond what information is directly represented. The fact that the results obtained with the expert description adhere to the content of the description itself is a highly desirable feature for controllable music

Model	H_{inst}	H_{chord}
Ground truth	3.763	4.077
Huang et al. (2018)	3.251	3.749
Choi et al. (2020)	3.647	3.949
Wu & Yang (2021)	1.804	2.420
FIGARO (expert)	3.732	4.049
FIGARO (learned)	3.825	4.085
FIGARO	3.661	4.071

Table 2. Instrument entropy H_{inst} and chord entropy H_{chord} for ground truth and modelled distributions. Model entropies are empirical estimates over samples from the conditional generation task. Closest to ground truth is best.

generation. By using this description, the degree of control exerted by the user is enhanced and the results match expectations. We also observe that adding learned features further improves performance across the board, with FIGARO beating FIGARO (expert) in every category. The success of this hybrid approach means that we can preserve the interpretability and inductive bias, yet increase the quality of the generated music by exploiting black-box AI.

Our expert description and hybrid models significantly outperform all baselines, and the learned description model outperforms Choi et al. (2020) on most metrics by a slight margin. The difference in performance is explained by the conditioning used for Choi et al. (2020), where the conditioning vector is temporally aggregated over the entire sample with any style progression throughout the sequence being lost. Wu & Yang (2021) attempt to alleviate this problem by deriving the conditioning vector from the current bar and varying it over time. However, the model experiences posterior collapse in our experiments when trained on the diverse LakhMIDI dataset, which is apparent by the low entropy of the model distribution (see Table 2) as well as the worse-than-unconditional performance on some description metrics. The full list of results is provided in Table 3a.

6.2. Zero-Shot Medley Generation

We evaluate the out-of-distribution performance of our models by combining two sequences $\mathbf{x}^{(1)}$ and $\mathbf{x}^{(2)}$ into a new sequence that does not belong to the training distribution. To this end, we take 16 bars of each sequence and concatenate them to form a novel sequence $\tilde{\mathbf{x}} = b_1^{(1)} \parallel \dots \parallel b_{16}^{(1)} \parallel b_{17}^{(2)} \parallel \dots \parallel b_{32}^{(2)}$. We then feed the description $F(\tilde{\mathbf{x}})$ into the model and iteratively sample the output distribution to generate a "medley" of the input sequences. We use the same models as for the conditional generation task without further fine-tuning or other modifications. We omit Huang et al. (2018) and Wu & Yang (2021) from the comparison as we do not expect competitive performance based on the results of the conditional generation task.

Model	Fluency PPL ↓	Accuracy			Fidelity					
		I ↑	C ↑	TS ↑	ND ↓	P ↑	V ↑	D ↑	s_c ↑	s_g ↑
Huang et al. (2018)	1.988	0.191	0.048	0.751	2.192	0.563	0.153	0.312	0.306	0.510
Choi et al. (2020)	2.049	0.658	0.184	0.908	1.679	0.646	0.574	0.484	0.514	0.688
Wu & Yang (2021)	2.094	0.179	0.050	1.000	0.873	0.492	0.050	0.207	0.312	0.529
FIGARO (expert)	1.913	0.957	0.561	0.996	0.319	0.759	0.658	0.514	0.712	0.637
FIGARO (learned)	1.973	0.594	0.195	0.969	0.738	0.701	0.653	0.546	0.544	0.697
FIGARO	1.705	0.960	0.593	0.997	0.238	0.827	0.735	0.748	0.790	0.853

(a) Conditional generation perplexity and similarity metrics. Best values are highlighted.

Model	Fluency PPL ↓	Accuracy			Fidelity					
		I ↑	C ↑	TS ↑	ND ↓	P ↑	V ↑	D ↑	s_c ↑	s_g ↑
Choi et al. (2020)	2.213	0.441	0.129	0.808	1.407	0.603	0.396	0.448	0.437	0.643
FIGARO (expert)	1.824	0.944	0.524	0.992	0.384	0.741	0.559	0.497	0.705	0.575
FIGARO (learned)	2.186	0.381	0.128	0.829	0.831	0.649	0.424	0.478	0.446	0.614
FIGARO	1.782	0.917	0.514	0.988	0.335	0.807	0.702	0.694	0.748	0.744

(b) Zero-shot medley generation perplexity and similarity metrics. Best values are highlighted.

Model	Fluency PPL ↓	Accuracy			Fidelity					
		I ↑	C ↑	TS ↑	ND ↓	P ↑	V ↑	D ↑	s_c ↑	s_g ↑
FIGARO (expert)	1.894	0.955	0.553	0.996	0.360	0.700	0.646	0.434	0.710	0.639
- w/o instruments	1.980	0.373	0.568	1.000	0.424	0.674	0.586	0.436	0.687	0.625
- w/o chords	2.023	0.895	0.100	0.995	0.564	0.672	0.603	0.413	0.294	0.615
- w/o meta information	1.966	0.908	0.536	0.795	0.878	0.574	0.205	0.334	0.636	0.584

(c) Ablation study perplexity and similarity metrics. Worst values are emphasized.

Table 3. We compare our models to the unconditional baseline based on Huang et al. (2018) and MuseMorphose (Wu & Yang, 2021) on perplexity (PPL) and similarity metrics. Similarity metrics include instrument F_1 -score (I), chord F_1 -score (C) and time signature accuracy (TS) as well as note density NRMSE (ND), pitch MOA (P), velocity MOA (V), duration MOA (D), chroma similarity s_c and grooving similarity s_g .

We see a drop in performance in all evaluation metrics for every model compared to the conditional generation task, which is expected due to distributional shifts in the data. However, models using the expert description as input drop significantly less than FIGARO (learned) and Choi et al. (2020). This shows that the expert description provides a strong inductive bias and is robust with respect to distributional shifts, which is not the case for other models. We sometimes even observe FIGARO turning the hard cut-off points from bar-splicing into smooth transitions, which can be attributed to its capacity to pay attention to future bars and anticipate a significant change in style. The perplexity of FIGARO (expert) even improves over the conditional generation task, which might be caused by noise but could also be another indication for good generalization. The complete list of results is available in Table 3b.

6.3. Ablation Study

To evaluate which parts of the expert description are essential, we group it into three components: instruments, chords and meta-information. Instruments and chords include all tokens with information about instruments and chords re-

spectively while all other tokens (time signature, note density and mean pitch, velocity and duration) are classified as meta-tokens. We train separate models with one part of the description removed and compare the performance to FIGARO (expert), which receives the full expert description as input.

As one would expect, removing each component reduces the performance significantly in the respective metrics, indicating that each component carries useful information not entirely inferable through the remaining components. Interestingly, our experiments show that removing any component slightly decreases the over-all performance even in metrics that we would not necessarily expect to be affected. Removing instrument information, for example, increases the error for note density, pitch, velocity and duration, indicating that the instruments also carry implied information about those features. This seems plausible considering the fact that different styles (or genres) of music usually identifies a set of instruments that is common for said style. Similar arguments can be made for the other two components. The full list of results is available in Table 3c.

6.4. Subjective Evaluation

Finally, we evaluate the subjective quality of generated samples through a user study, comparing our best model to the baselines. To this end, we have conducted a survey where participants were asked to indicate their preference between 20 second excerpts of two samples chosen uniformly at random. In total, we gathered 7569 comparisons by 691 unique participants. In two types of questions, participants had to choose 1) between a real sample and a generated sample or 2) between two generated samples.

Question type 1) ranks the different methods on how good generated samples are compared to real, human-composed music. In this respect, FIGARO beats all other baseline with a win rate of 39.3% compared to the next best model by Huang et al. (2018), which has a win rate of 33.2%. Win rates of the different models are displayed in Figure 4 with 90% confidence intervals obtained through normal approximation. While Choi et al. (2020) is able to adhere to the prescribed condition as shown in Section 6.1, the quality of generated samples is approximately on par with the unconditional model. FIGARO on the other hand is able to surpass the unconditional baseline in sample quality, while providing controllable generation capabilities.

Question type 2) is used to construct a pairwise ranking of models by applying the Wilcoxon signed-rank test on the study results. In this ranking, our model beats each of the baselines with a p -value of $< 10^{-7}$. The complete ranking and test results can be found in Appendix E.

7. Discussion

7.1. Future Work

While our work represents a step towards high-quality controllable symbolic music generation, we recognize several avenues for future work. The proposed model is good at adhering to the prescribed description and generating music that is similar to the input overall, but some salient features such as melodies are often not preserved. This can be explained by a lacking bias toward reconstructing melodies accurately, which may be remedied by introducing melody-focused descriptions or auxiliary loss functions.

Furthermore, the design space for description functions is largely left unexplored. It is worth investigating whether using different functions leads to vastly different results. While we show that each component of the expert description is essential, we have no rigorous nor empirical evidence that the features we chose to use are optimal.

Finally, as the description-to-sequence objective is not exclusively applicable to symbolic music, it will be interesting to apply this method to different data. For example, the long-range conditioning ability could potentially allow for

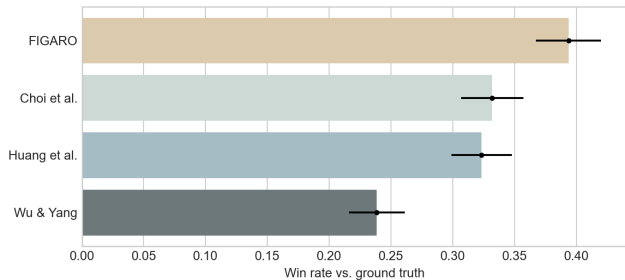


Figure 4. Win rates of generated samples against real samples. We compare FIGARO, Huang et al. (2018), Choi et al. (2020) and Wu & Yang (2021). Real samples are from the test set.

generating natural language that is coherent for much longer passages as well as allowing the user to define a story progression or over-arching structure.

7.2. Conclusion

We present the description-to-sequence objective as a self-supervised modelling task and apply it in the context of symbolic music generation. We propose FIGARO, which combines two description functions in a model that enables fine-grained, global control over the generation process. To the best of our knowledge, our method is the first that can generate symbolic music based on user-provided sequence-level guidelines. In terms of sample quality, our method beats other state-of-the-art symbolic music generative models trained on the LakhMIDI dataset. The proposed description functions each have their own strengths: The expert description is a human-interpretable sequence that is easy to create and edit and acts as a strong inductive bias to the model. The learned description allows for more high-fidelity, detailed information to be expressed in the description while sacrificing human-interpretable. We can combine both approaches to achieve human-interpretable, high fidelity controllable symbolic music generation.

On a broader perspective, we hope that the proposed method is a step toward facilitating artists in their creative process as well as enabling amateurs to express themselves by lowering the barrier of entry to music creation and making the process faster and easier overall.

Ethical Considerations

Automatic music generation may raise ethical concerns similar to those of large language models. The models may exhibit biases toward a certain style of music and may not represent the music of marginalized cultures accurately. In our case, the majority of training samples are western music, which is not necessarily representative of music at large. The model might also reproduce copyrighted material that is present in the training data and potentially generate samples that infringe on copyright law.

References

- Baevski, A., Schneider, S., and Auli, M. vq-wav2vec: Self-Supervised Learning of Discrete Speech Representations. In *International Conference on Learning Representations*, September 2019. URL <https://openreview.net/forum?id=rylwJxrYDS>.
- Biggio, L., Bendinelli, T., Neitz, A., Lucchi, A., and Parascandolo, G. Neural symbolic regression that scales. In Meila, M. and Zhang, T. (eds.), *Proceedings of the 38th International Conference on Machine Learning*, volume 139 of *Proceedings of Machine Learning Research*, pp. 936–945. PMLR, 18–24 Jul 2021. URL <https://proceedings.mlr.press/v139/biggio21a.html>.
- Brown, T. B., Mann, B., Ryder, N., Subbiah, M., Kaplan, J., Dhariwal, P., Neelakantan, A., Shyam, P., Sastry, G., Askell, A., Agarwal, S., Herbert-Voss, A., Krueger, G., Henighan, T., Child, R., Ramesh, A., Ziegler, D. M., Wu, J., Winter, C., Hesse, C., Chen, M., Sigler, E., Litwin, M., Gray, S., Chess, B., Clark, J., Berner, C., McCandlish, S., Radford, A., Sutskever, I., and Amodei, D. Language models are few-shot learners, 2020.
- Brunner, G., Konrad, A., Wang, Y., and Wattenhofer, R. MIDI-VAE: Modeling Dynamics and Instrumentation of Music with Applications to Style Transfer. In *arXiv:1809.07600 [cs, eess, stat]*, September 2018. URL <http://arxiv.org/abs/1809.07600>. arXiv: 1809.07600.
- Choi, K., Hawthorne, C., Simon, I., Dinculescu, M., and Engel, J. Encoding Musical Style with Transformer Autoencoders. In *Proceedings of the 37th International Conference on Machine Learning*, pp. 1899–1908. PMLR, November 2020. URL <https://proceedings.mlr.press/v119/choi20b.html>. ISSN: 2640-3498.
- Devlin, J., Chang, M.-W., Lee, K., and Toutanova, K. BERT: Pre-training of Deep Bidirectional Transformers for Language Understanding. *arXiv:1810.04805 [cs]*, May 2019. URL <http://arxiv.org/abs/1810.04805>. arXiv: 1810.04805.
- Dhariwal, P., Jun, H., Payne, C., Kim, J. W., Radford, A., and Sutskever, I. Jukebox: A Generative Model for Music. *arXiv:2005.00341 [cs, eess, stat]*, April 2020. URL <http://arxiv.org/abs/2005.00341>. arXiv: 2005.00341.
- Di, S., Jiang, Z., Liu, S., Wang, Z., Zhu, L., He, Z., Liu, H., and Yan, S. Video Background Music Generation with Controllable Music Transformer. In *Proceedings of the 29th ACM International Conference on Multimedia*, pp. 2037–2045, October 2021. URL <https://doi.org/10.1145/3474085.3475195>.
- Dixon, S., Gouyon, F., and Widmer, G. Towards Characterisation of Music via Rhythmic Patterns. *ISMIR*, 2004.
- Dosovitskiy, A., Beyer, L., Kolesnikov, A., Weissenborn, D., Zhai, X., Unterthiner, T., Dehghani, M., Minderer, M., Heigold, G., Gelly, S., Uszkoreit, J., and Houselby, N. An Image is Worth 16x16 Words: Transformers for Image Recognition at Scale. *arXiv:2010.11929 [cs]*, June 2021. URL <http://arxiv.org/abs/2010.11929>. arXiv: 2010.11929.
- Ens, J. and Pasquier, P. Quantifying Musical Style: Ranking Symbolic Music based on Similarity to a Style. *ISMIR*, November 2019. URL <https://archives.ismir.net/ismir2019/paper/000107.pdf>.
- Ens, J. and Pasquier, P. MMM : Exploring Conditional Multi-Track Music Generation with the Transformer. *arXiv:2008.06048 [cs]*, August 2020. URL <http://arxiv.org/abs/2008.06048>. arXiv: 2008.06048.
- Ferreira, L. N. and Whitehead, J. Learning to Generate Music With Sentiment. *arXiv:2103.06125 [cs, eess]*, March 2021. URL <http://arxiv.org/abs/2103.06125>. arXiv: 2103.06125.
- Fujishima, T. Real-time chord recognition of musical sound: A system using common lisp music. In *Proc. ICMC, Oct. 1999*, pp. 464–367, 1999.
- Hadjeres, G. and Crestel, L. Vector Quantized Contrastive Predictive Coding for Template-based Music Generation. *arXiv:2004.10120 [cs, eess]*, April 2020. URL <http://arxiv.org/abs/2004.10120>. arXiv: 2004.10120.
- Hernandez-Olivan, C. and Beltran, J. R. Music Composition with Deep Learning: A Review. *arXiv:2108.12290 [cs, eess]*, September 2021. URL <http://arxiv.org/abs/2108.12290>. arXiv: 2108.12290.
- Hsiao, W.-Y., Liu, J.-Y., Yeh, Y.-C., and Yang, Y.-H. Compound Word Transformer: Learning to Compose Full-Song Music over Dynamic Directed Hypergraphs. *arXiv:2101.02402 [cs, eess]*, January 2021. URL <http://arxiv.org/abs/2101.02402>. arXiv: 2101.02402.
- Huang, C.-Z. A., Vaswani, A., Uszkoreit, J., Shazeer, N., Simon, I., Hawthorne, C., Dai, A. M., Hoffman, M. D., Dinculescu, M., and Eck, D. Music Transformer. *arXiv:1809.04281 [cs, eess, stat]*, December 2018. URL <http://arxiv.org/abs/1809.04281>. arXiv: 1809.04281.

- Huang, Y.-S. and Yang, Y.-H. Pop Music Transformer: Beat-based Modeling and Generation of Expressive Pop Piano Compositions. *arXiv:2002.00212 [cs, eess, stat]*, August 2020. URL <http://arxiv.org/abs/2002.00212>. arXiv: 2002.00212.
- Huang, Z., Liang, D., Xu, P., and Xiang, B. Improve Transformer Models with Better Relative Position Embeddings. *arXiv:2009.13658 [cs]*, September 2020. URL <http://arxiv.org/abs/2009.13658>. arXiv: 2009.13658.
- Kaiser, Ł., Roy, A., Vaswani, A., Parmar, N., Bengio, S., Uszkoreit, J., and Shazeer, N. Fast Decoding in Sequence Models using Discrete Latent Variables. *arXiv:1803.03382 [cs]*, June 2018. URL <http://arxiv.org/abs/1803.03382>. arXiv: 1803.03382.
- Karras, T., Laine, S., and Aila, T. A Style-Based Generator Architecture for Generative Adversarial Networks. *arXiv:1812.04948 [cs, stat]*, March 2019. URL <http://arxiv.org/abs/1812.04948>. arXiv: 1812.04948.
- Kingma, D. P. and Ba, J. Adam: A Method for Stochastic Optimization. *arXiv:1412.6980 [cs]*, January 2017. URL <http://arxiv.org/abs/1412.6980>. arXiv: 1412.6980.
- Lample, G. and Charton, F. Deep learning for symbolic mathematics, 2019.
- Nierhaus, G. Historical Development of Algorithmic Procedures. In *Algorithmic Composition: Paradigms of Automated Music Generation*, pp. 7–66. Springer, Vienna, 2009. ISBN 978-3-211-75540-2. doi: 10.1007/978-3-211-75540-2.2. URL https://doi.org/10.1007/978-3-211-75540-2_2.
- Oord, A. v. d., Vinyals, O., and Kavukcuoglu, K. Neural Discrete Representation Learning. *arXiv:1711.00937 [cs]*, May 2018. URL <http://arxiv.org/abs/1711.00937>. arXiv: 1711.00937.
- Oord, A. v. d., Li, Y., and Vinyals, O. Representation Learning with Contrastive Predictive Coding. *arXiv:1807.03748 [cs, stat]*, January 2019. URL <http://arxiv.org/abs/1807.03748>. arXiv: 1807.03748.
- Payne, C. MuseNet, April 2019. URL <https://openai.com/blog/musenet/>.
- Raffel, C. *Learning-Based Methods for Comparing Sequences, with Applications to Audio-to-MIDI Alignment and Matching*. PhD thesis, Columbia University, 2016.
- Ramesh, A., Pavlov, M., Goh, G., Gray, S., Voss, C., Radford, A., Chen, M., and Sutskever, I. Zero-Shot Text-to-Image Generation. *arXiv:2102.12092 [cs]*, February 2021. URL <http://arxiv.org/abs/2102.12092>. arXiv: 2102.12092.
- Shao, B., Li, T., and Ogihara, M. Quantify music artist similarity based on style and mood. In *Proceedings of the 10th ACM workshop on Web information and data management, WIDM '08*, pp. 119–124, New York, NY, USA, October 2008. Association for Computing Machinery. ISBN 978-1-60558-260-3. doi: 10.1145/1458502.1458522. URL <https://doi.org/10.1145/1458502.1458522>.
- Vaswani, A., Shazeer, N., Parmar, N., Uszkoreit, J., Jones, L., Gomez, A. N., Kaiser, Ł., and Polosukhin, I. Attention is All you Need. In *Advances in Neural Information Processing Systems*, pp. 5998–6008. Curran Associates, Inc., 2017.
- Wu, S.-L. and Yang, Y.-H. MuseMorphose: Full-Song and Fine-Grained Music Style Transfer with Just One Transformer VAE. *arXiv:2105.04090 [cs, eess]*, May 2021. URL <http://arxiv.org/abs/2105.04090>. arXiv: 2105.04090.

A. REMI+ Input Representation

We extend the original REMI representation (Huang & Yang, 2020) to make it suitable for general multi-track, multi-signature symbolic music sequences. We make modifications that add time signature and instrument information, we determine a unique order of events and use quantization schemes that allow for accurate representation for a diverse set of music. An example of a REMI+ sequence is given in Figure 5.

Bar Tokens. To provide the model with additional context, we include the index of the current bar in each bar token. This, along with the bar embedding, should help the model retrieve the correct information from the description and help determine the end of a piece at generation time.

Time signature. We add a time signature token at the beginning of each bar, indicating the time signature of the bar which is to follow. We adapt the convention that time signature changes may only happen at the beginning of a bar, which is commonly true in written music.

Instruments. We add instrument information as an additional token before each note event, indicating which instrument will play the following note.

Order of events. In theory, the order of notes within each bar can be arbitrary without compromising the validity of the sequence. But to make the modelling task easier, we define a unique and deterministic order of events. Specifically, we sort events by (Bar, Position, EventType, Instrument, Pitch) in ascending order (valid event types are {Chord, Tempo, Note}). This order is unique since a given instrument can only ever play a single note with a given pitch at a given time³.

Quantization. We largely follow Huang & Yang (2020) in quantization. The most significant deviation is the use of 12 note onset positions per quarter note instead of 4 as proposed in the original work. For example, there will be 48 unique note onset positions for the 4/4 time signature and 36 note onset positions for the 3/4 time signature. This allows both triplet and sixteenth notes to be quantized accurately, which is important when considering a diverse set of music.

Instruments and note pitches are not quantized as they are categorical variables with 128 possible values by the MIDI specification. Note velocity is quantized to 32 intervals in $[0, 128]$ and note duration is quantized to position intervals defined by the following mesh:

$$\begin{aligned} \mathcal{M} = & \{1, \dots, 12\} \cup \\ & \{12 + 3i \mid i \in (1, \dots, 4)\} \cup \\ & \{12 + 4i \mid i \in (1, \dots, 3)\} \cup \\ & \{24 + 6i \mid i \in (1, \dots, 4)\} \cup \\ & \{48 + 12i \mid i \in (1, \dots, 12)\} \cup \\ & \{192 + 24i \mid i \in (1, \dots, 24)\} \end{aligned}$$

This ensures single position accuracy up to quarter notes, then 16th and triplet accuracy up to half notes and 8th note accuracy up to a full note. To limit vocabulary size, we switch to quarter note steps up to 8 full notes and half note steps up to 16 full notes after that. Notes longer than 16 full notes are truncated to this length. Finally, tempo change events are discretized to 32 intervals in $[0, 240]$.

```
<bos>
Bar_1 TimeSignature_3/4
  Pos_0 Tempo_120
  Pos_0 Chord_C:min
  Pos_0 Instrument_Drums Pitch_36 Vel_90 Dur_0
  Pos_0 Instrument_Piano Pitch_64 Vel_85 Dur_4
  Pos_4 Instrument_Piano Pitch_66 Vel_85 Dur_4
Bar_2 TimeSignature_3/4
  Pos_0 Tempo_120
  ...
<eos>
```

Figure 5. Example sequence represented in the REMI+ representation. At the beginning of each bar time signature, tempo and the current chord are noted, after which each note is represented through five subsequent tokens.

³This is an assumption that could be violated in theory but does hold in practice.

B. Expert Description Algorithm

Pseudocode for generating the expert description is given in Algorithm 1. We quantize note density, mean pitch and velocity to 32 linearly spaced intervals in $[0, 12]$, $[0, 128]$ and $[0, 128]$ respectively. Mean duration is quantized to 32 logarithmically spaced intervals in $[0, 128]$ positions (12 positions per quarter note).

Algorithm 1 ExpertDescription

```

input musical sequence  $\mathbf{x}$ 
output description  $\mathbf{d}$ 
 $\mathbf{d} \leftarrow ()$ 
 $b_1, \dots, b_n \leftarrow \text{PARTITIONINTOBARS}(\mathbf{x})$ 
for  $b_i \in (b_1, \dots, b_n)$  do
     $N \leftarrow \{n \mid n \text{ is a note with onset in } b_i\}$ 
     $I \leftarrow \{\text{inst} \mid \text{inst is being played during } b_i\}$ 
     $C \leftarrow \{\text{chord} \mid \text{chord is being played during } b_i\}$ 
     $q \leftarrow \text{duration of } b_i \text{ in quarter notes}$ 
     $\text{ts} \leftarrow \text{time signature at beginning of } b_i$ 
     $\text{nd} \leftarrow \frac{|N|}{q}$ 
     $\text{mp} \leftarrow \frac{1}{|N|} \sum_{n \in N} \text{PITCH}(n)$ 
     $\text{mv} \leftarrow \frac{1}{|N|} \sum_{n \in N} \text{VELOCITY}(n)$ 
     $\text{md} \leftarrow \frac{1}{|N|} \sum_{n \in N} \text{DURATION}(n)$ 
    Quantize  $\text{nd}, \text{mp}, \text{mv}$  and  $\text{md}$ 
     $d_i \leftarrow (i, \text{ts}, \text{nd}, \text{mp}, \text{mv}, \text{md}) \parallel \text{list}(I) \parallel \text{list}(C)$ 
     $\mathbf{d} \leftarrow \mathbf{d} \parallel d_i$ 
end for
return  $\mathbf{d}$ 
    
```

C. Evaluation Metrics

C.1. Macro Overlapping Area

As used by previous work, the overlapping area (OA) metric does not consider the sequential order of the investigated feature, as feature histograms are computed over the entire sequence. For example, the overlapping area of \mathbf{x} and $\text{reverse}(\mathbf{x})$ would be maximal, even though the reversed sequence does not sound like the original sequence in general.

To alleviate this limitation, we adapt the OA metric to also consider temporal order. Let \mathbf{x} and \mathbf{y} denote two musical sequences and let $b_i^{(\mathbf{x})}$ and $b_i^{(\mathbf{y})}$ denote the i -th bar of \mathbf{x} and \mathbf{y} respectively. We compute the overlap in feature distributions for each bar by fitting a Gaussian distribution to the feature under examination (e.g. note pitch) and compute the overlapping area between the two distributions. Let this overlap be given by $\text{overlap}(b_i^{(\mathbf{x})}, b_i^{(\mathbf{y})})$. Then the macro overlapping area (MOA) between \mathbf{x} and \mathbf{y} is given by

$$\text{MOA}(\mathbf{x}, \mathbf{y}) = \frac{1}{N} \sum_{i=1}^N \text{overlap}(b_i^{(\mathbf{x})}, b_i^{(\mathbf{y})})$$

C.2. Normalized Root-Mean-Square Error

In order to normalize for different feature magnitudes between different samples, we compute the normalized RMSE (NRMSE) for bar-wise note density. Let x denote the ground truth, \hat{x} denote the reconstruction and N denote the length of

the sequences. Then the NRMSE is given by

$$\text{RMSE}(x, \hat{x}) = \sqrt{\frac{1}{N} \sum_{i=1}^N (\hat{x}_i - x_i)^2}$$

$$\text{NRMSE}(x, \hat{x}) = \frac{\text{RMSE}(x, \hat{x})}{\text{mean}(x)}$$

C.3. Cosine Similarity

Let $\mathbf{v}_i^{(x)}$ and $\mathbf{v}_i^{(y)}$ denote the chroma vector (Fujishima, 1999) or grooving vector (Dixon et al., 2004) for the i -th bar in \mathbf{x} and \mathbf{y} respectively. We then average the cosine similarity over the entire sequence to get the chroma/grooving similarity:

$$\text{sim}_{\mathbf{v}}(\mathbf{x}, \mathbf{y}) = \frac{1}{N} \sum_{i=1}^N \frac{\mathbf{v}_i^{(x)} \cdot \mathbf{v}_i^{(y)}}{\|\mathbf{v}_i^{(x)}\| \|\mathbf{v}_i^{(y)}\|}$$

D. Benchmark Models

D.1. Huang et al. (2018)

We reimplement the model proposed by Huang et al. (2018) as an unconditional baseline. We train the model on the REMI+ representation to allow for direct comparison to our method. We use the improved relative attention from Huang et al. (2020) to eliminate any possible advantage arising from different attention mechanisms. We largely stick to the hyperparameters from our models, using 6 decoder layers with a hidden size of 512 and a filter size of 2048. Training and optimization hyperparameters are also the same as for our models.

D.2. Choi et al. (2020)

We reimplement the model proposed by Choi et al. (2020) and train it on the REMI+ representation to allow for direct comparison to our method. We again use the improved relative attention from Huang et al. (2020) and largely stick to the hyperparameters from the original paper, using 6 encoder and 6 decoder layers. Unlike the original work, we do not use data augmentation since the dataset is large enough and in order to allow for fair comparison between the models. Due to GPU memory constraints we reduce the context size from 2048 to 1024 and use an accumulated batch size of 16, ensuring stable training. Training and optimization hyperparameters are the same as for our models.

D.3. Wu & Yang (2021)

We train MuseMorphose on the REMI+ representation to allow for direct comparison to our method. Adapting the released implementation for our experiments, we reduce the context size from 1280 to 512 tokens due to GPU memory constraints but leave all other hyperparameters as they were proposed in the original paper. The model is trained until convergence (approx. 125k steps). We limit the training data to a subset of the entire dataset (20k samples) due to technical limitations. This is still considerably more training data than what was used in the original paper (1k samples) and should not affect performance significantly compared to using the full dataset.

E. Subjective Evaluation

The study includes 7569 comparisons by 691 participants, each averaging 11 answers. In each comparison, participants were presented with two different samples and were asked to indicate, which of the two they preferred. For the following ranking test, samples were chosen uniformly at random from two different generative models, the pair of which again was chosen at random. In this setup, we treat real samples as one possible model, for which we simply sample the test distribution. For the other models, we generate samples as described for the conditional generation task (Section 6.1).

We apply the Wilcoxon signed-rank test to the results in order to establish a ranking of the different models. FIGARO beats each baseline except ground truth with a win rate of more than 60% and a p -value of less than 10^{-7} . Out of all methods, FIGARO also has the highest win rate against real samples with a win rate of 39.3%, which is a 6% advantage over the next best method. Rankings and corresponding p -values are reported in Table 4.

Model	Opponent	Winrate	p -value	N
1. Ground truth		0.669		2418
	FIGARO	0.605	$< 10^{-6}$	595
	Huang et al. (2018)	0.663	$< 10^{-15}$	605
	Choi et al. (2020)	0.647	$< 10^{-12}$	586
	Wu & Yang (2021)	0.756	$< 10^{-37}$	632
2. FIGARO		0.581		2439
	Huang et al. (2018)	0.609	$< 10^{-7}$	635
	Choi et al. (2020)	0.624	$< 10^{-9}$	631
	Wu & Yang (2021)	0.696	$< 10^{-20}$	578
3. Huang et al. (2018)		0.463		2467
	Choi et al. (2020)	0.543	0.0162	613
	Wu & Yang (2021)	0.581	$< 10^{-4}$	614
4. Choi et al. (2020)		0.447		2490
	Wu & Yang (2021)	0.589	$< 10^{-5}$	660
5. Wu & Yang (2021)		0.345		2484

Table 4. Ranking of the different methods by winrate according to the user study. The Wilcoxon signed-rank test is used to calculate pairwise ranking p -values. "Ground truth" denotes sampling the test set.